JACS
JOURNAL OF THE AMERICAN CHEMICAL SOCIETY

Communication

pubs.acs.org/JACS

# Tunable Localized Surface Plasmon Resonances in Tungsten Oxide Nanocrystals

Karthish Manthiram[†,§] and A. Paul Alivisatos*[,‡,§]

[†]Department of Chemical Engineering and [‡]Department of Chemistry, University of California, Berkeley, California 94720, United States

[§]Materials Sciences Division, Lawrence Berkeley National Laboratory, Berkeley, California 94720, United States

Supporting Information

**ABSTRACT:** Transition-metal oxide nanocrystals are interesting candidates for localized surface plasmon resonance hosts because they exhibit fascinating properties arising from the unique character of their outer-d valence electrons. $WO_{3-\delta}$ nanoparticles are known to have intense visible and near-IR absorption, but the origin of the optical absorption has remained unclear. Here we demonstrate that metallic phases of $WO_{3-\delta}$ nanoparticles exhibit a strong and tunable localized surface plasmon resonance, which opens up the possibility of rationally designing plasmonic tungsten oxide nanoparticles for light harvesting, bioimaging, and sensing.

Free charge carriers that are dielectrically confined to a nanoparticle at sufficient density participate in resonant, collective oscillations known as localized surface plasmon resonances (LSPRs). There is a dramatic enhancement in the optical field in the vicinity of a plasmonic nanoparticle, which provides for unprecedented control over light-induced excitations at length scales smaller than the diffraction limit. This control has led to the development of plasmonic nanoparticles tailored for applications as diverse as biosensing,[1] cancer photothermal therapy,[2] and light-harvesting in photovoltaics.[3]

The vast majority of investigations of LSPRs have been conducted on noble metals, as they are stable under a wide range of conditions and have a high charge carrier density. LSPRs have also been reported in heavily doped semiconductor nanocrystals, including tin oxide,[4] copper chalcogenides,[5] and zinc oxide.[6] LSPRs in heavily doped semiconductors are unique because the LSPR energy may be tuned by adjusting the doping or stoichiometry, providing an additional means of tuning the optical properties that is not as readily available in metals.[7]

Transition-metal oxides (TMOs) are interesting candidates for LSPR hosts because they exhibit fascinating properties arising from the unique character of the outer-d valence electrons.[8] Some of the hallmarks of TMOs include metal−insulator transitions, high-temperature superconductivity, fast ionic transport, and colossal magnetoresistance, which have led to unique applications in the areas of microelectronics, quantum computing, spintronics, and energy conversion and storage. We expect that the exotic properties of TMOs will lead to distinctive plasmonic effects at the nanoscale. For instance, metal−insulator transitions, which have been well-studied in TMOs, may be leveraged to generate LSPRs that are switchable in response to a variety of stimuli, including temperature, pressure, and composition. In fact, a temperature-switchable LSPR has been identified in vanadium dioxide.[9] An LSPR has also been identified in rhenium trioxide,[10] but the tunability of its charge carrier density has not been demonstrated; in addition, rhenium is among the most expensive metals, which limits practical applications.

Tungsten oxide nanocrystals are a system of particular interest for the study of tunable plasmon resonances in nanoparticles, as tungsten oxide is stable under a wide range of conditions and has a band gap of 2.6 eV, which is ideal for absorption of visible light. These properties have led to the use of tungsten oxide as an anode in photoelectrochemical cells for water splitting.[11] In the bulk, tungsten oxide exhibits a strong color change upon intercalation of small ions such as $Li^+$ or $H^+$ or due to oxygen deficiency.[12] In the case of $WO_{3-\delta}$, which generally has a strong blue color, a variety of oxygen-deficient stoichiometries can be obtained, e.g., $WO_{2.72}$ ($W_{18}O_{49}$), $WO_{2.8}$ ($W_5O_{14}$), $WO_{2.83}$ ($W_{24}O_{68}$), and $WO_{2.9}$ ($W_{20}O_{58}$). These are ordered phases with precise stoichiometries. For $0 < \delta < 0.1$ in bulk $WO_{3-\delta}$, the electrical and optical properties are dominated by localized electrons involved in polarons, which are quasiparticles consisting of a charge carrier and its polarization field in a lattice. Bulk $WO_{3-\delta}$ undergoes a metal−insulator transition at $\delta = 0.1$, as the localized polaronic wave functions begin to overlap and form delocalized states.[13] As a result, for $\delta > 0.1$ in bulk $WO_{3-\delta}$, the electrical and optical properties are dominated by free electrons. The metal−insulator transition has been firmly established in bulk $WO_{3-\delta}$ by a combination of temperature-dependent conductivity measurements,[14] reflectivity measurements of the bulk plasma frequency,[15] and X-ray photoelectron spectroscopy (XPS).[16] Thus, there is a wide range of known phenomena from the bulk that may exhibit interesting size- and shape-dependent behavior at the nanoscale.

To date, studies of nanoscale $WO_{3-\delta}$ have led to some contradictory results. For instance, $WO_{2.72}$ ($W_{18}O_{49}$) nanowires appear to be semiconducting on the basis of electrical transport[17] and photoluminescence studies;[18] it has been proposed that the blue color of nanoscale $WO_{2.72}$ may arise from polaron hopping. In contrast, $WO_{2.8}$ ($W_5O_{14}$) nanowires appear to be metallic on the basis of XPS and electrical

**Received:** December 5, 2011
**Published:** February 14, 2012

   dx.doi.org/10.1021/ja211363w | J. Am. Chem. Soc. 2012, 134, 3995−3998

transport measurements;[19] this material is also blue, but the origin of its optical absorption has not been discussed in the literature. We demonstrate in this communication that nanoscale $WO_{2.83}$ ($W_{24}O_{68}$) can support strong LSPRs and that these LSPRs account for a strong absorption feature ranging from the red edge of the visible to the near-IR (NIR).

$WO_{2.83}$ nanorods were prepared by hot injection of tungsten(V) ethoxide into a solvent mixture of oleic acid and trioctylamine at 315 °C under an inert atmosphere [see the Supporting Information (SI)].[20] The recovered product exhibited a strong blue color (Figure 1a). Transmission

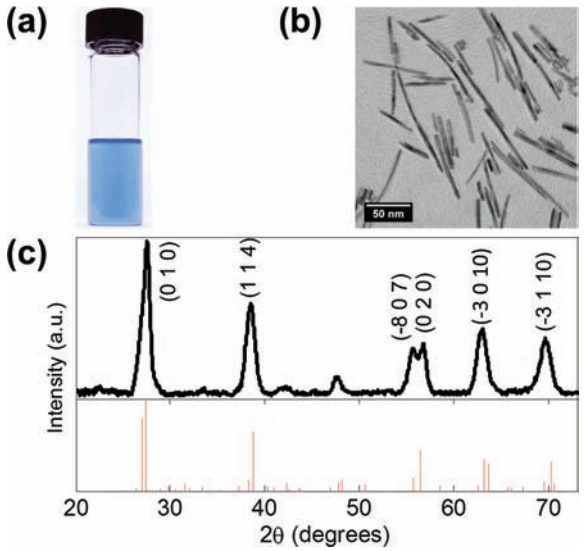


**Figure 1.** (a) Photograph of $WO_{2.83}$ nanorods in *N*-methylpyrrolidone. (b) TEM micrograph of $WO_{2.83}$ nanorods. (c) XRD pattern of $WO_{2.83}$ nanorods (top) and the reference pattern for $WO_{2.83}$ (bottom).

electron microscopy (TEM) revealed a rodlike morphology (Figure 1b) with an average width of 5.4 nm and an average length of 62 nm (see the SI). X-ray diffraction (XRD) demonstrated that the particles have the monoclinic structure of $W_{24}O_{68}$ (Figure 1c), which corresponds to a stoichiometry of $WO_{2.83}$.[21] Like many nonstoichiometric TMOs, $WO_{3-\delta}$ has rich phase behavior, and the particular phase that is obtained depends significantly on the synthetic conditions used.

The optical absorption spectrum of our $WO_{2.83}$ nanorods has a peak centered at approximately 900 nm (Figure 2a). We used Mie–Gans theory[22] to predict the LSPR spectrum that we would expect for our $WO_{2.83}$ nanorods. The LSPR absorbance $A$ of a solution of nanorods is given by

$$A \propto \omega \varepsilon_m^{3/2} \sum_j \frac{\left(\frac{1}{P_j^2}\right)\varepsilon_2}{\left(\varepsilon_1 + \frac{1-P_j}{P_j}\varepsilon_m\right)^2 + \varepsilon_2^2} \tag{1}$$

where $\omega$ is the angular frequency of incident light, $\varepsilon_m$ is the dielectric constant of the medium, $\varepsilon_1$ and $\varepsilon_2$ are the real and imaginary parts, respectively, of the dielectric function $\varepsilon(\omega)$ of $WO_{2.83}$, and the $P_j$ are the depolarization factors for axes A, B, and C of the rod (A is the long axis, while B and C are the short

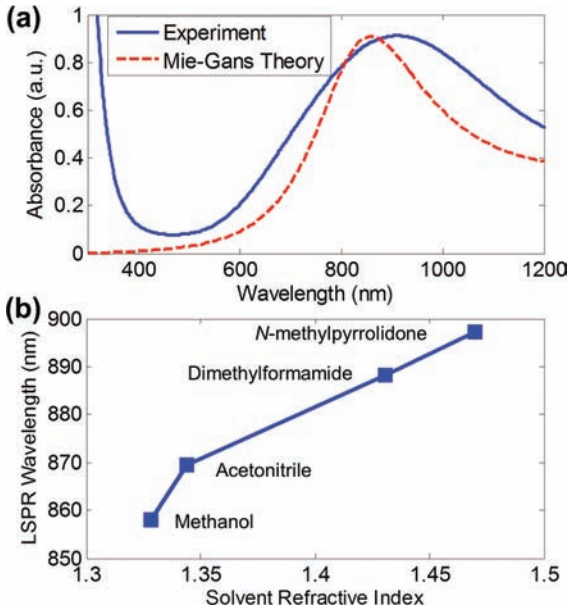


**Figure 2.** (a) Comparison of experimentally observed and theoretically predicted absorption spectra of the short-axis mode of $WO_{2.83}$ rods in *N*-methylpyrrolidone. (b) Experimentally observed short-axis LSPR wavelength as a function of the refractive index of the solvent.

axes). We assume that axes B and C have the same width for a rod. The depolarization factors in eq 1 are given by

$$P_A = \frac{(1-s^2)}{s^2}\left[\frac{1}{2s}\ln\left(\frac{1+s}{1-s}\right) - 1\right] \tag{2}$$

$$P_B = P_C = \frac{(1-P_A)}{2} \tag{3}$$

The geometric parameter $s$ that appears in eq 2 is

$$s = \sqrt{1 - \left(\frac{1}{R}\right)^2} \tag{4}$$

where $R$ is the aspect ratio of the rods. We approximate the dielectric function $\varepsilon(\omega)$ of $WO_{2.83}$ in eq 1 as that of a free-electron gas in the energy range of interest:

$$\varepsilon(\omega) = \varepsilon_1 + i\varepsilon_2 = 1 - \frac{\omega_p^2}{\omega^2 + i\gamma\omega} \tag{5}$$

where $\omega_p$ is the bulk plasma frequency and $\gamma$ is the collision frequency. The bulk plasma frequency $\omega_p$ in eq 5 is

$$\omega_p = \sqrt{\frac{Ne^2}{\varepsilon_0 m_e}} \tag{6}$$

where $N$ is the charge carrier density, $e$ is the elementary charge, $\varepsilon_0$ is the permittivity of free space, and $m_e$ is the effective mass of an electron. The collision frequency $\gamma$ in eq 5 is given by

$$\gamma = \frac{1}{\tau} = \frac{e^2}{\sigma m_e} \tag{7}$$

where $\tau$ is the scattering time of an electron and $\sigma$ is the conductivity. We had to estimate several of the parameters in the above equations in order to calculate the LSPR spectrum of


dx.doi.org/10.1021/ja211363w | J. Am. Chem. Soc. 2012, 134, 3995–3998

our $WO_{2.83}$ nanorods. From the TEM images of our nanorods, we know that the aspect ratio is $R = 11$ (see the SI). If it is assumed that each oxygen vacancy generates two electrons, the charge carrier density in $WO_{2.83}$ is $N = 6.3 \times 10^{21}$ cm$^{-3}$. The effective mass of $WO_{3-\delta}$ has been found to be in the range of $m_0$ to $1.4m_0$, where $m_0$ is the rest mass of an electron; hence, we used $m_e = 1.2m_0$.[23] The conductivity of $WO_{2.83}$ has been previously measured to be $\sigma = 2 \times 10^3\ \Omega^{-1}$ cm$^{-1}$.[13]

Using eq 1, the parameters defined in eqs 2−7, and the above assumptions, we calculated the absorption spectrum of $WO_{2.83}$ nanorods (Figure 2a). We found that Mie−Gans theory predicted the short-axis mode of $WO_{2.83}$ nanorods in *N*-methylpyrrolidone to occur at a wavelength of 860 nm, which is remarkably close to the experimentally observed wavelength of 900 nm. We expect that the experimentally observed short-axis mode is broader than predicted by Mie−Gans theory because of sample inhomogeneity and damping of the plasmon arising from surface scattering of electrons.[24] In a rod-shaped sample, the long-axis mode is ordinarily the easier mode to observe because of strong coupling to the electromagnetic field. However, in this case, the absorption due to the long-axis mode is expected to occur at very low energy and to be quite broad, rendering it difficult to observe; in fact, our calculations suggested that for a high enough aspect ratio, the long-axis mode does not exhibit a maximum in absorption (see the SI). In contrast, the short-axis mode is quite strong and readily observable in the NIR to visible regime.

The observed decrease in the LSPR energy with increasing refractive index of the medium is consistent with what we would expect for an LSPR (Figure 2b). The magnitude of the experimentally observed shift in the LSPR energy as the solvent was changed from methanol to *N*-methylpyrrolidone was 40 nm, which is smaller than the shift of 60 nm predicted using eq 1. This is reasonable since the solvent may not have complete access to the surface of the particle because of ligand coverage, leading to a weaker dependence of the LSPR energy on the solvent refractive index. Chemical interactions between the solvent and nanoparticle surface can also contribute to differences between the experimental and theoretical LSPR shifts. The complex effect of steric and chemical interactions on the magnitude of the LSPR shift has been well-established for gold nanoparticles.[25] In addition, if some population of electrons are still involved in a polaronic transition,[13] there may be a polaronic contribution to the optical absorption in $WO_{2.83}$, which would also reduce the magnitude of the observed shift in the LSPR energy.

The plasmon energy of $WO_{2.83}$ particles could be tuned by heating in an oxidizing environment. When a solution of particles in *N*-methylpyrollidone was heated at 175 °C in air, we observed a red shift and a decrease in the intensity of the plasmon (Figure 3a). We expect that the plasmon is red shifted and reduced in intensity as a result of the incorporation of oxygen into the lattice, leading to a decrease in the carrier concentration. We did not observe the same effect when the solution was heated under an argon atmosphere, suggesting that oxygen plays a key role in this process. The observed blue shift in the band-gap absorption upon heating (Figure 3a) is also consistent with oxygen incorporation, as it has been previously observed that the band gap of $WO_{3-\delta}$ is blue-shifted with decreasing $\delta$. XRD of the heated particles suggested that they have a disordered structure (Figure 3b), which demonstrates that although oxygen may enter the structure at a low temperature and annihilate the charge carrier, the particles do not fully retain their crystallinity. The disorder may also decrease the effective mass of the electron, further red-shifting the LSPR energy.

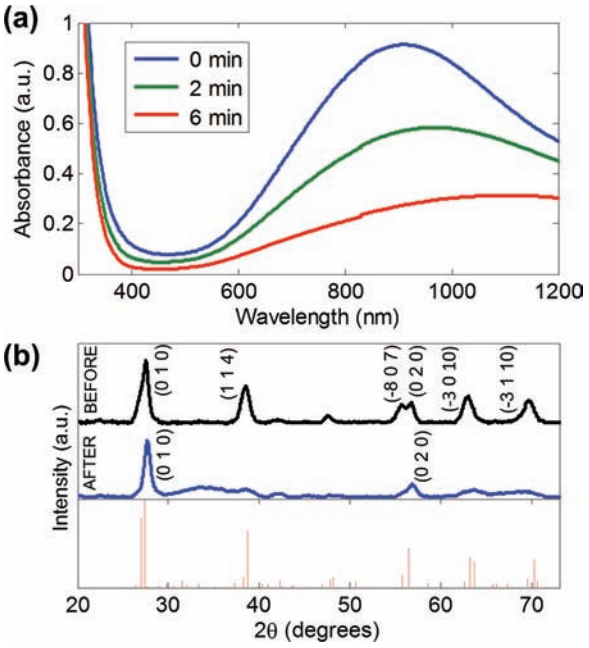


**Figure 3.** (a) UV−vis−NIR absorption spectra of $WO_{2.83}$ nanorods in *N*-methylpyrrolidone upon heating at 175 °C in air for 0, 2, and 6 min. (b) XRD patterns of $WO_{2.83}$ nanorods in *N*-methylpyrrolidone (top) before and (middle) after heating at 175 °C for 6 min in air and (bottom) the reference pattern for $WO_{2.83}$.

The short-axis mode of the $WO_{2.83}$ nanorods exhibited a high plasmonic sensitivity of 280 nm per refractive index unit (nm/RIU), which is comparable to those of silver nanoprisms (200 nm/RIU for prisms of 50 nm height and 100 nm width),[26] gold nanoshells (130 to 360 nm/RIU for nanoshell thickness to core radius ratios of 3 to 0.1, respectively),[27] and spherical $Cu_{2-x}S$ (350 nm/RIU).[5] Normalizing the plasmonic sensitivity by the LSPR line width gave a sensing figure of merit of 0.5. The quality factor, defined as the ratio of the LSPR energy to the line width, was 1.6, which is less than those of gold and silver nanostructures.[28] The quality factor serves as an indicator of the local electric field enhancement. As a result, the electric field in the vicinity of a $WO_{2.83}$ nanoparticle is expected to be weaker than those of gold and silver nanoparticles.

The high energy of the $WO_{2.83}$ LSPR relative to other identified semiconductor LSPRs, which arises from the high charge carrier density of $N = 6.3 \times 10^{21}$ cm$^{-3}$, opens up many practical applications for semiconductor plasmons in the areas of bioimaging, sensing, and light harvesting. The plasmon energy of $WO_{2.83}$ is especially desirable for in vivo bioimaging, as it falls in the "therapeutic window" in which light has a large penetration depth in tissue.[29] In addition, nanostructured $WO_{3-\delta}$ has been investigated for gas sensing applications, as the selectivity for various gases can be tuned by adjusting the stoichiometry of $WO_{3-\delta}$.[30] With increasing interest in the use of nanostructured tungsten oxide as an anode in photoelectrochemical cells, it will be important to pay attention to how oxygen deficiency impacts its photocatalytic properties. Previous studies have used nanostructured $WO_{3-\delta}$ for photocatalysis, as it is stable under photocatalytic conditions and its band gap may be tuned by changing the stoichiometry.[31] The new understanding of the LSPR mode present in $WO_{2.83}$ may


dx.doi.org/10.1021/ja211363w | *J. Am. Chem. Soc.* 2012, 134, 3995−3998

provide a better understanding of these previous results and enable the rational design of new plasmonically enhanced tungsten oxide nanostructures for bioimaging, sensing, and light harvesting.

## ■ ASSOCIATED CONTENT

### Supporting Information

Synthesis and characterization methods, absorption calculations, high-resolution TEM images, and particle size distributions. This material is available free of charge via the Internet at http://pubs.acs.org.

## ■ AUTHOR INFORMATION


### Corresponding Author

alivis@berkeley.edu


### Notes

The authors declare no competing financial interest.

## ■ ACKNOWLEDGMENTS

We thank B. Beberwyck, D. Britt, C. Choi, D. Grauer, P. K. Jain, M. Lucas, Y. Surendranath, and J. Wang for useful discussions and advice. This work was supported by the Joint Center for Artificial Photosynthesis, a DOE Energy Innovation Hub funded by the Office of Science of the U.S. Department of Energy under Award DE-AC02-05CH11231. K.M. gratefully acknowledges the support of the Department of Energy Office of Science Graduate Fellowship Program (DOE SCGF), made possible in part by the American Recovery and Reinvestment Act of 2009 and administered by ORISE−ORAU under Contract DE-AC05-06OR23100.

## ■ REFERENCES


(1) Jain, P. K.; Huang, X.; El-Sayed, I. H.; El-Sayed, M. A. *Plasmonics* **2007**, *2*, 107.

(2) West, J. L.; Halas, N. J. *Annu. Rev. Biomed. Eng.* **2003**, *5*, 285.

(3) Atwater, H. A.; Polman, A. *Nat. Mater.* **2010**, *9*, 205.

(4) (a) Nutz, T.; Felde, U.; Haase, M. *J. Chem. Phys.* **1999**, *110*, 12142. (b) Kanehara, M.; Koike, H.; Yoshinaga, T.; Teranishi, T. *J. Am. Chem. Soc.* **2009**, *131*, 17736. (c) Garcia, G.; Buonsanti, R.; Runnerstrom, E. L.; Mendelsberg, R. J.; Llordes, A.; Anders, A.; Richardson, T. J.; Milliron, D. J. *Nano Lett.* **2011**, *11*, 4415. (d) Li, S. Q.; Guo, P.; Zhang, L.; Zhou, W.; Odom, T. W.; Seideman, T.; Ketterson, J. B.; Chang, R. P. H. *ACS Nano* **2011**, *5*, 9161.

(5) (a) Zhao, Y.; Pan, H.; Lou, Y.; Qiu, X.; Zhu, J.; Burda, C. *J. Am. Chem. Soc.* **2009**, *131*, 4253. (b) Luther, J. M.; Jain, P. J.; Ewers, T.; Alivisatos, A. P. *Nat. Mater.* **2011**, *10*, 361. (c) Dorfs, D.; Hartling, T.; Miszta, K.; Bigall, N. C.; Kim, M. R.; Genovese, A.; Falqui, A.; Povia, M.; Manna, L. *J. Am. Chem. Soc.* **2011**, *133*, 11175. (d) Kriegel, I.; Jiang, C.; Rodriguez-Fernandez, J.; Schaller, R. D.; Talapin, D. V.; Como, E.; Feldmann, J. *J. Am. Chem. Soc.* **2012**, *134*, 1583.

(6) Buonsanti, R.; Llordes, A.; Aloni, S.; Helms, B.; Milliron, D. J. *Nano Lett.* **2011**, *11*, 4706.

(7) Boltasseva, A.; Atwater, H. A. *Science* **2011**, *331*, 290.

(8) Goodenough, J. B. *Prog. Solid State Chem.* **1971**, *5*, 145.

(9) Rini, M.; Cavalleri, A.; Schoenlein, R. W.; Lopez, R.; Feldman, L. C.; Haglund, R. F.; Boatner, L. A.; Haynes, T. E. *Opt. Lett.* **2005**, *30*, 558.

(10) Biswas, K.; Rao, C. N. R. *J. Phys. Chem. B* **2006**, *110*, 842.

(11) Hodes, G.; Cahen, D.; Manassen, J. *Nature* **1976**, *260*, 312.

(12) Deb, S. K. *Sol. Energy Mater. Sol. Cells* **1992**, *25*, 327.

(13) Salje, E.; Guttler, B. *Philos. Mag. B* **1984**, *50*, 607.

(14) Sahle, W.; Nygren, M. *J. Solid State Chem.* **1983**, *48*, 154.

(15) Viswanathan, K.; Brandt, K.; Salje, E. *J. Solid State Chem.* **1981**, *36*, 45.

(16) Gehlig, R.; Salje, E. *J. Solid State Chem.* **1983**, *49*, 318.

(17) Shi, S.; Xue, X.; Feng, P.; Liu, Y.; Zhao, H.; Wang, T. *J. Cryst. Growth* **2008**, *310*, 462.

(18) Su, C.-Y.; Lin, H.-C. *J. Phys. Chem. C* **2009**, *113*, 4042.

(19) Remskar, M.; Kovac, J.; Virsek, M.; Mrak, M.; Jesih, A.; Seabaugh, A. *Adv. Funct. Mater.* **2007**, *17*, 1974.

(20) Yella, A.; Tahir, M. N.; Meuer, S.; Zentel, R.; Berger, R.; Panthöfer, M.; Tremel, W. *J. Am. Chem. Soc.* **2009**, *131*, 17566.

(21) Booth, J.; Ekstrom, T.; Iguchi, E.; Tilley, R. J. D. *J. Solid State Chem.* **1982**, *41*, 293.

(22) Link, S.; Mohamed, M. B.; El-Sayed, M. A. *J. Phys. Chem. B* **1999**, *103*, 3073.

(23) Molenda, J.; Kubik, A. *Phys. Status Solidi* **1995**, *191*, 471.

(24) Alvarez, M. M.; Khoury, J. T.; Schaaff, T. G.; Shafigullin, M. N.; Vezmar, I.; Whetten, R. L. *J. Phys. Chem. B* **1997**, *101*, 3706.

(25) Ghosh, S. K.; Nath, S.; Kundu, S.; Esumi, K.; Pal, T. *J Phys. Chem. B* **2004**, *108*, 13963.

(26) Malinsky, M. D.; Kelly, K. L.; Schatz, G. C.; Van Duyne, R. P. *J. Am. Chem. Soc.* **2001**, *123*, 1471.

(27) Jain, P. K.; Huang, W.; El-Sayed, M. A. *J. Phys. Chem. C* **2007**, *111*, 17451.

(28) Sonnichsen, C.; Franzl, T.; Wilk, T.; Plessen, G.; Feldman, J. *Phys. Rev. Lett.* **2002**, *88*, 77402.

(29) Richards-Kortum, R.; Sevick-Muraca, E. *Annu. Rev. Phys. Chem.* **1996**, *47*, 555.

(30) Berger, O.; Hoffman, T.; Fischer, W.-J. *J. Mater. Sci.* **2004**, *15*, 483.

(31) Sun, S.; Chang, X.; Dong, L.; Zhang, Y.; Li, Z.; Qiu, Y. *J. Solid State Chem.* **2011**, *184*, 2190.